

CFD Analysis of Blood Flow Obstruction in Coronary Arteries and Its Impact on Heart Blockages

Manoj A. Kumbhalkar ^{1*}, Tukaram S. Sargar ², Nitin B. Kardekar ¹, Suhas H. Sarje ³, Sunil Prayagi ⁴,
Gaurav Gondhlekhar ⁵, Kunal Jadhav ¹

¹ Department of Mechanical Engineering, JSPM Narhe Technical Campus, Pune, India

² Department of Mechanical Engineering, Smt. Kashibai Navale College of Engineering, Pune, India

³ Department of Mechanical Engineering, Jayawatrao Sawant College of Engineering, Pune, India

⁴ Department of Mechanical Engineering, Yeshwantrao Chavan College of Engineering, Nagpur, India.

⁵ Department of Electrical Engineering, Yeshwantrao Chavan College of Engineering, Nagpur, India,

*Corresponding author E-mail: manoj.kumbhalkar@rediffmail.com

Received: April 3, 2025, Accepted: July 3, 2025, Published: July 18, 2025

Abstract

Blood vessels, which are veins and arteries, are the high-speed highways employing muscular pumps to propel blood throughout the body. Any disease or clot within the blood vessels that interrupt the pathway of blood flow stops the smooth flow of the blood, thus changing the hemodynamic of the blood. That creates a condition that is fatal. The hemodynamic mechanism of a portion of a stiffened coronary artery resulting from sudden obstruction or stagnant flow, and the interrelation between rheological and mechanical parameters in vascular occlusion such as velocity and pressure. For various vascular occlusion sizes and blockages case studies, the oscillation pressure, pressure profile and velocity of blood through artery have been analysed and discussed. Changes in the pressure of blood flow through the arterial wall create stress. These walls of the artery contract and expand as the blood pressure increases when this pressure falls. In the case study of the patient blockage within an artery, the principal aims of the simulation were to find the velocity, pressure, and wall shear stress when there is an artery blockage. The ANSYS Design Modeller program and Computational Fluid Dynamics method is employed to simulate and analyse the blood artery with various sizes of vascular occlusion. CFD analysis proves that the blood flows smoothly and also pressure is reduced for blockages under sub-arteries. The pressure for the case of blockages at the beginning of artery and before sub-artery is more for the condition of 81% block and may be a condition of fatal. Computational Fluid Dynamics-based blood vessel simulation gives crucial information for the diagnosis of the circulatory barrier.

Keywords: Arteries, Left coronary artery, Blockages, Ansys CFD Fluent.

1. Introduction

Recent advances in computational fluid dynamics (CFD) have made it possible to model the cardiovascular (CV) system's blood flow. The computer can display the blood flow pattern for different diseased arteries. As a result, CFD is being used as a clinical diagnosis tool for vascular disorders in medical practice across the region. It is possible to increase artery blood flow by applying the physical laws.

High mortality rates are caused by cardiovascular diseases (CDs), which are brought on by people's poor habits and sedentary lifestyles in the twenty-first century. CDs are a group of heart and blood vascular illnesses. According to India's current heart disease statistics, around 17.5 million people pass away from CDs every year. The treatment of CDs is one of the main causes for concern because, at the current rate, heart problems in India are expected to reach an alarming height by 2020. The vast vascular network of elastic muscles in the human body facilitates the flow of blood to bodily tissues. Any aberrant change in blood vessel geometry alters the regular blood flow pattern, which over time leads to heart-related illnesses or heart attacks. The aorta is the main blood conduit that emerges from the left ventricle of the heart and uses the heart's pumping mechanism to carry blood to other body parts. It is a three-dimensional, curving tube-like structure made up of the descending limb, aortic arch, and ascending limb. Because of the pulsatile character of blood flow and geometric differences such as strength, curvature, torsion, tapering, bending, and branching, the development of flow in the aorta is complicated.

For the diagnosis and treatment of CDs such as aneurysm, atherosclerosis, arteriosclerosis, stenosis, etc., CFD has several uses. Coronary artery disease is caused by atherosclerosis. The slow accumulation of plaque in your body's arteries is known as atherosclerosis. You have coronary artery disease when the plaque in your coronary arteries interferes with blood flow.

Calcium, waste materials, cholesterol, and fibrin—a material that aids in blood clotting—make up plaque. Your arteries narrow and stiffen as plaque keeps building up along their walls. Blood flow to a particular area of your body may be restricted or stopped by plaque that clogs or damages your arteries. Plaque accumulation in the coronary arteries prevents enough blood from reaching the heart muscle. Thus,

your heart is unable to receive the oxygen and nutrients it requires for optimal function. We refer to this condition as myocardial ischemia. It increases your risk of having a heart attack and causes angina or chest pain.

Plaque accumulation in the coronary arteries frequently occurs in other parts of the body as well. Conditions like peripheral artery disease and carotid artery disease may result from this.

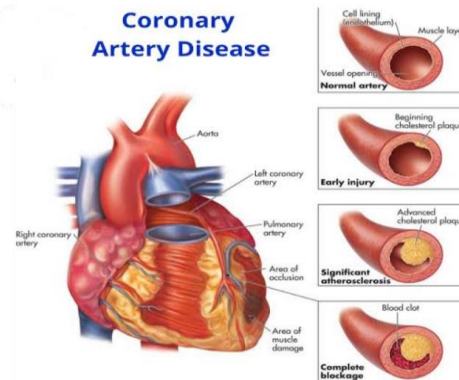


Fig. 1: Arteries with Plaque Formation [18]

Arteries are blood veins that transport blood from the heart. The arteries transport the lungs' highly oxygenated blood to the body's tissues. This rule is completely broken by the pulmonary artery and the pulmonary circulation loop trunk, which transport deoxygenated blood to the lungs where it is oxygenated by the heart. Because arteries bear most of the power that the blood exerts after leaving the heart, blood pressure is high in the arteries. Compared to vein walls, artery walls are thicker, more muscular, and more elastic. Greater elastic tissues found in larger arteries enable them to expand and withstand the elevated cardiac pressure.

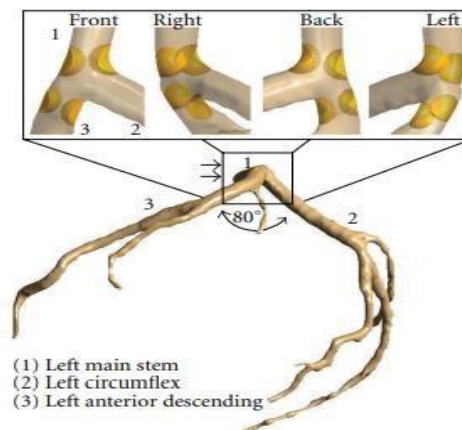


Fig. 2: Plaque distribution in left coronary artery [2]

The study aims to analyze blood velocity, wall pressure, and blood flow changes in the human body, which cannot be directly measured in blood vessels. Computational Fluid Dynamics (CFD) serves as an alternative method for diagnosing coronary artery disease (CAD), as wall shear stress plays a critical role in the formation and development of atherosclerotic plaques. The objectives of the study include analyzing patient angiography with medical consultation, examining oscillating pressure, pressure drop, and blood flow velocity in blocked arteries, assessing pressure drop variations for different blockage sizes, and conducting CFD analysis considering the properties of blood flow through arteries. The scope of the study highlights that angiography detects blockages, while CFD tools help determine pressure and velocity in the affected areas, assisting medical officers in correlating findings with ECG results for necessary interventions. The methodology consists of six phases. Phase I involves analytically calculating pressure and velocity at the blockage using the continuity and Bernoulli equations. Phase II consists of developing a 2D sample model in AutoCAD and the simulation of water flowing through a blocked pipe, with velocity analysis performed in ANSYS CFD Fluent. Phase III includes analyzing patient angiography reports and comparing blocked arteries. Phase IV includes designing case models in PTC Creo 10, as per research parameters, with three different blockage placement models. Phase V uses CFD analysis through ANSYS 22 with meshing, inlet and outlet blood flow setup, and mechanical parameters derived from research studies and fluid dynamics libraries. Finally, in Phase VI, the process is validated through velocity and pressure drop measurement over arterial blockages, and then a complete report on CFD analysis results.

2. Related Work

The review of literature points towards different research papers on Computational Fluid Dynamics (CFD) simulation of blood flow in arteries with a focus on its importance to comprehend and diagnose cardiovascular diseases. Dwidmuthe et al. (2018) considered blood flow in the aorta as an unsteady and complex process affected by geometric characteristics like curvature and pulsatile nature. The research reconstructed the 3D geometry from MRI and conducted CFD simulations using blood as a Newtonian fluid and examined flow patterns, velocity, and wall shear stress (WSS). Chaichana et al. (2012) examined the hemodynamic influence of simulated plaques in left coronary arteries. The research compared Newtonian and non-Newtonian fluid models, emphasizing the relationship between coronary plaques and hemodynamic changes, especially pressure gradient (PSG) and flow velocities. Hannun and Muhseen (2020) simulated hemodynamic

characteristics in the right coronary artery with a non-Newtonian model of blood. Their CFD analysis showed elevated velocity in narrow diameters and changes in WSS distribution from the tilted axial velocity profile. Sahu et al. (2021) compared velocity, pressure, and WSS across various stages of blockage, simulating 10% to 80% blockages with different Reynolds numbers. Their research sought to learn about the effects of shear stress on essential organs and contribute to the creation of medical devices to minimize mortality rates. Carvalho et al. (2021) examined computational methods for modeling blood flow in diseased and normal arteries. Their research centered on models of blood viscosity, physiological conditions of flow, and the development of atherosclerosis, all contributing to enhanced diagnosis and treatment using numerical methods. Jameela et al. (2018) examined hemodynamic alterations in stiffened coronary arteries as a result of abrupt occlusions. ANSYS Design Modeler and CFD techniques were used by them to examine oscillating pressure, velocity, and WSS for various clot forms with their application for circulatory blockage diagnosis. Doost et al. (2016) explored patient-specific left ventricular (LV) simulations based on IB-CFD approaches over a period of 15 years. They segregated cases into pathological and physiological conditions, examining intraventricular flows and their application in cardiology. Their research focused on the significance of CFD for simulating real hemodynamics to assess clinical heart function. Such studies together serve as a sound basis for this work, accentuating the utility of CFD in diagnosing and comprehending hemodynamic alteration caused by artery blockage.

Morris et al. (2015) also surveyed the approach, advantages, and limitations of implementing CFD in cardiovascular medicine. Their work highlighted CFD's application in simulating blood flow, supporting medical device development, and facilitating patient-specific risk analysis and virtual treatment planning. Barzegar et al. (2021) studied the influence of blood flow rate on bifurcated arteries based on CFD simulations with the aim of determining the effect of artery angles on flow patterns and the contribution of fat accumulation in the blockage of arteries. Long et al. (2021) simulated blood flow behavior through consecutive series of clots within vessels, examining flow velocity distribution and stress changes through numerical solutions of Navier–Stokes equations. The research concluded that shear stress becomes much greater at increased blockage rates, and it influences the dynamics of blood flow. Pandey et al. (2019) conducted a simulation of blood flow through human coronary arteries with CFD and images obtained from angiography. They reconstructed a 3D model of 50% plaque blockage in the left coronary artery and compared velocity and wall shear stress under various flow conditions. Sheth and Ritter (2010) investigated the effect of stenting on blood flow velocity and proposed that elevated velocity after stenting could be due to decreased arterial wall compliance. They also related Doppler velocity measurements with the severity of stenosis to support treatment planning. Kim et al. (2010) created a model for predicting coronary flow and pressure by coupling 3D coronary artery models with heart and arterial system interaction. Their research gave realist coronary flow and pressure waveforms, facilitating better cardiovascular simulations.

The summary of the literature review highlights that CFD enables a better understanding of atherosclerosis, with factors such as velocity, pressure, and wall shear stress significantly affected at plaque locations. The studies indicate that velocity, pressure drop, and wall shear stress increase linearly with clot thickness, while the skin friction coefficient also rises correspondingly. These insights contribute to improving diagnosis, prognosis, and treatment planning for coronary artery diseases.

3. Modelling Of the Coronary Arteries

3.1 Case Study

For the blood flow analysis in the blockage of arteries, an angiography of the patient has been studied in consultation with the medical officer. In the below figure which is the left anterior descending artery in the heart having 35% blockages is considered for the analysis. The blockage area is shown in figure 3.

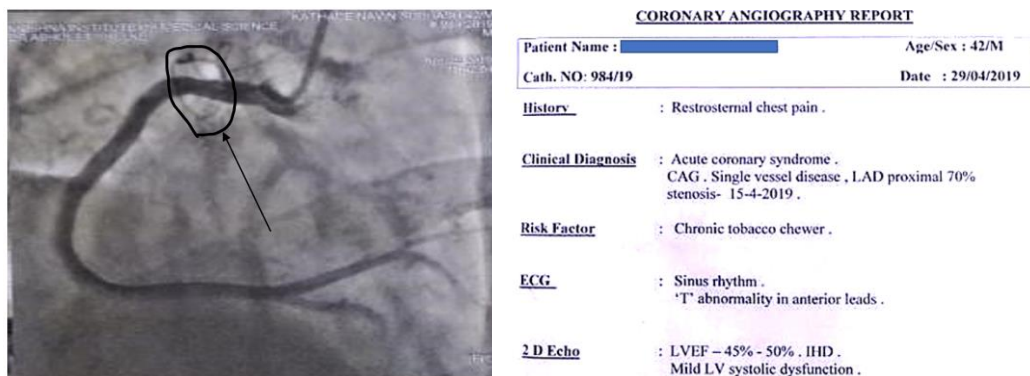


Fig. 3: Case study of blockage and Angiography result of case study

Patients frequently use the term "heart blockage" to describe coronary artery disease, a buildup of plaque that narrows the arteries supplying blood to the heart muscle. If the heart blockage is significant enough, it may prevent the muscle from receiving the blood it needs to operate, particularly during periods of exercise or other situations where increased blood flow is necessary. Breathlessness and chest pain are among the symptoms that result from this.

Nuclear scans and exercise stress tests are two of the tests that can be used to determine whether any parts of the heart have impaired blood flow. However, these tests are not ideal, and in patients who are found to be at high risk, a procedure known as a coronary angiography is used to examine the real vessel's outline in order to directly measure the heart blockage.

The heart receives its blood supply from three arteries that cross its surface. There are two arteries on the left side and one on the right. The right coronary is the one on the right. The left anterior descending (LAD), which flows along the front of the heart and serves the front and main wall, and the left circumflex, which provides the sidewall and major artery known as the left main artery, are located on the left side, or main side.

In certain instances, the percentage of blockages varies.

3.1.1 Case 1: Blockage 20 – 40%

The percentage of blockages in the artery is between 20 and 40 percent. Heart obstruction that is less than 40% is usually referred to as modest. It is quite improbable that such blockages produce symptoms because they are obviously not limiting blood flow. It is crucial to remember that there is unmistakable evidence of progressive coronary artery disease in these patients, and they require aggressive attention to coronary disease risk factors (such as blood pressure, smoking, cholesterol, and diabetes), the right medications, and healthy lifestyle modifications like exercise, dieting, and changing one's diet.

3.1.2 Case 2: Blockage 40 – 70%

As seen in Figure 4, where there is a 50% blockage at the start of the right coronary artery, a moderate degree of cardiac blockage is usually in the 40–70% range. In most cases, minor heart blockage does not result in symptoms since it does not significantly restrict blood flow. Treatment for moderate coronary artery disease is much the same as that for mild disease; it involves modifying one's lifestyle, taking medication, and paying attention to risk factors. Heart blockage at the upper end of the moderate range (50–70%) can occur sometimes.

3.1.3 Case 3: Blockage 70+%

Usually, a cardiac blockage that is more than 70% is considered severe. Shortness of breath and chest pain may be caused by this degree of constriction, which is linked to a markedly decreased blood supply to the heart muscle. Blockage is visible at the vessel's inception in 80% of cases. In reality, this is a bypass graft in a patient who has had bypass surgery. A stent was inserted into the obstruction to alleviate the symptoms of the severe heart blockage.

3.1.4 Case 3: Blockage 100%

A heart attack results from a complete blockage at the start of the right coronary artery, which stops blood flow further. Significant symptoms are usually present with such a cardiac obstruction, and prompt treatment is required. Stent placement was used to restore normal blood flow to this artery, as seen in the image. If medication is not administered promptly (generally within the first few hours, the sooner the better), the heart muscle may die and, once dead, is typically not able to recover, leading to heart failure and decreased heart pumping capacity.

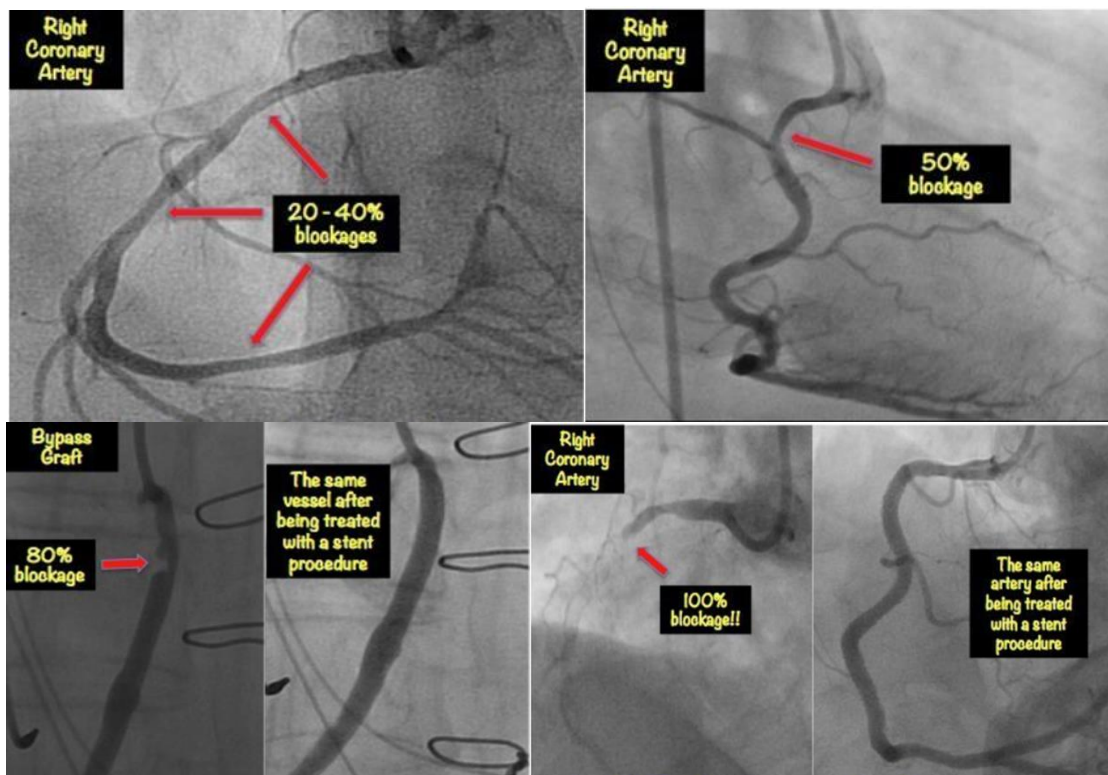


Fig. 4: Coronary artery scan with blockages from 20% to 100%

3.2 Models with Blockage

3.2.2 Case Model

The CAD model is created with Creo software, the model parameter is taken from the paper Journal of Hypertension and Cardiology. From it the diameter of the left coronary artery was found in the range between 1.20- 4.70mm. The tetrahedral meshing is created to the model and boundary conditions are applied (Inlet, Outlet, Wall).

The below figure 5, It is cut section of the LAD artery, which shows as it is effect of the case with 35% blockage.

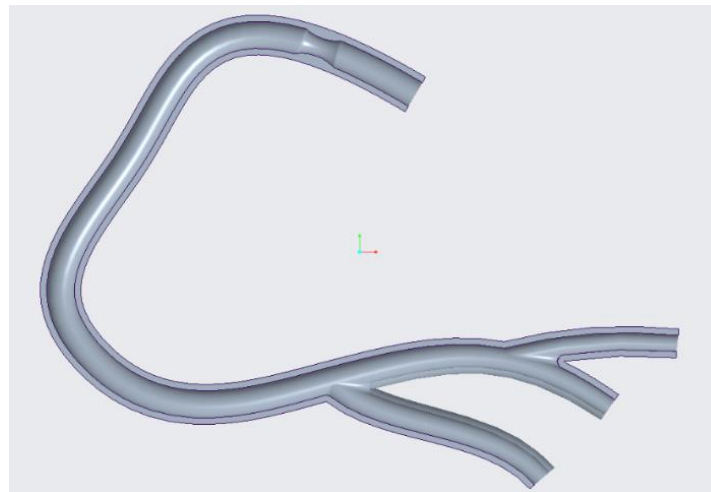


Fig. 5: Blockage at the beginning of Left Anterior Descending (LAD) artery

Various design models were created by varying the percentages of blockages in the artery, considering blockage levels of 81%, 61%, 48%, 35%, and 19%. In the model with 81% blockage in the Left Anterior Descending (LAD) artery, the diameter of the artery is 3.1 mm, with a central diametrical distance of 0.6 mm and a blockage length of 2.5 mm. The 61% blockage model possesses a central diametrical distance of 1.2 mm and a blockage length of 1.9 mm. Likewise, in the 48% blockage model, the central diametrical distance is raised to 1.6 mm with a blockage length of 1.5 mm. In the 35% blockage model, the central diametrical distance is elevated to 2.0 mm and the blockage length to 1.1 mm. Finally, the 19% blockage model has the minimum restriction, with the central diametrical distance being 2.5 mm and blockage length being 0.6 mm. These models permit CFD analysis to study the influence of different blockages on parameters like blood velocity, pressure drop, and wall shear stress, assisting in coronary artery disease evaluation as well as assisting medical personnel in diagnosis and treatment planning.

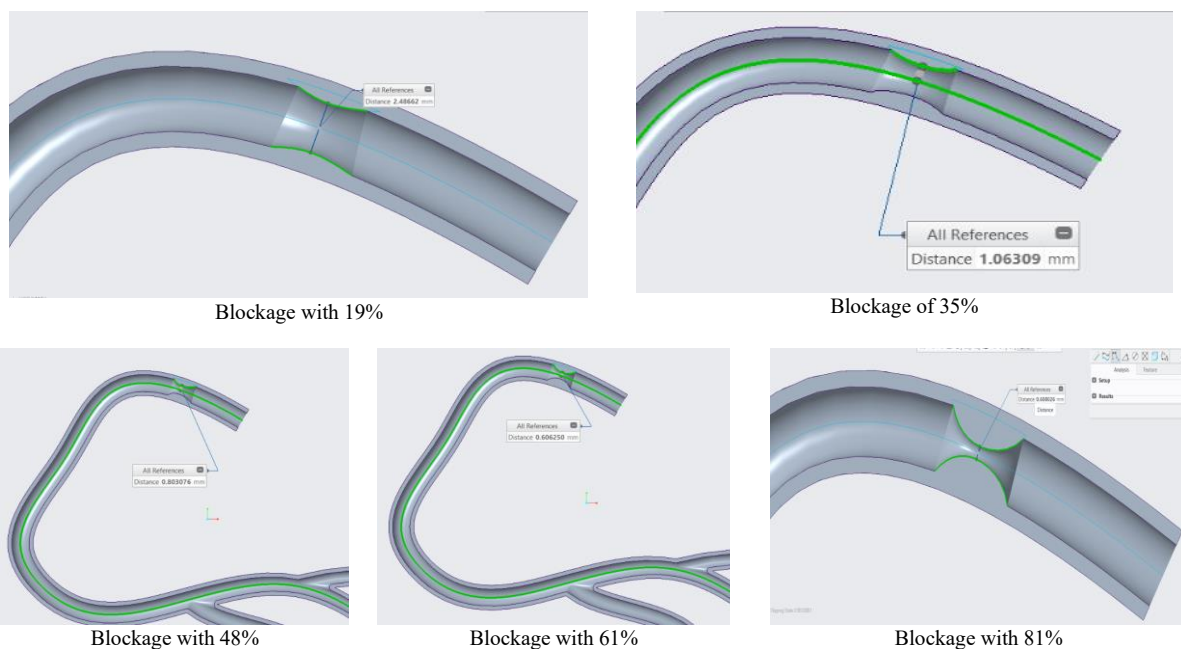


Fig. 6: Design models for varying percentages of blockages at the beginning of artery, considering blockage levels of 81%, 61%, 48%, 35%, and 19%.

Table 1 shows the various types of models, dimensions and its blockages percentages.

Table 1: Percentages of Blockages at beginning of artery and before sub-artery

Diameter of Artery	3.1 mm		
Design Model	Diameter Gap	Blockage	Percentage of Block
LAD_ 0.6 mm	0.6	2.5	81
LAD_ 1.2 mm	1.2	1.9	61
LAD_ 1.6 mm	1.6	1.5	48
LAD_ 2.0 mm	2.0	1.1	35
LAD_ 2.5 mm	2.5	0.6	19

3.2.3 Case 2

The diameter of the artery is 3.1 mm, and blockages are placed before the branches as shown in the Figure 7.



Fig. 7: Blockage in Left Anterior Descending (LAD) artery before sub-arteries

Various arterial blockage models were designed to analyze the impact of different levels of stenosis on blood flow dynamics. The 81% blockage model considers an arterial diameter of 3.1 mm, with a central diametrical distance of 0.6 mm and a blockage length of 2.5 mm. In the 61% blockage model, the central diametrical distance increases to 1.2 mm, while the blockage length is reduced to 1.9 mm. The 48% blockage model enhances the central diametrical distance to 1.6 mm with a 1.5 mm blockage length. Also, in the 35% blockage model, the central diametrical distance is 2.0 mm with a 1.1 mm blockage length. Finally, the 19% blockage model is the least severe condition, with a 2.5 mm central diametrical distance and a 0.6 mm blockage length. These models offer a systematic method for computational fluid dynamics (CFD) analysis, allowing one to better comprehend how different degrees of arterial blockage affect major hemodynamic parameters like velocity, pressure drop, and wall shear stress.

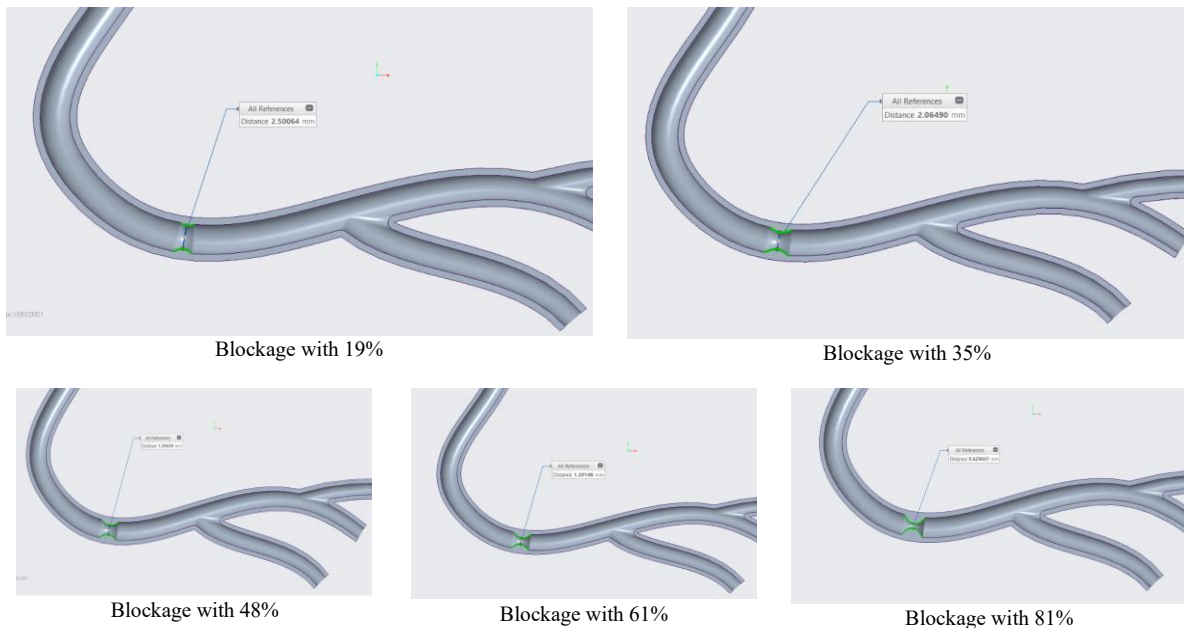


Fig. 8: Design models for varying percentages of blockages before sub-arteries, considering blockage levels of 81%, 61%, 48%, 35%, and 19%.

3.2.4 Case 3

Table 2 shows the model with changed position of blockages, after the branches with 5 model.

Table 2: The blockage under sub-arteries.

Diameter of Artery	2.84 mm		
Design Model	Diameter Gap	Blockage	Percentage of Block
LAD 0.55 mm	0.55	2.29	81
LAD 1.1 mm	1.1	1.74	61
LAD 1.45 mm	1.47	1.37	48
LAD 1.8 mm	1.85	0.99	35
LAD 2.25 mm	2.29	0.55	19

The diameter of the artery is 2.84 mm, and blockages are placed after the branches, which is shown in Figure 9.

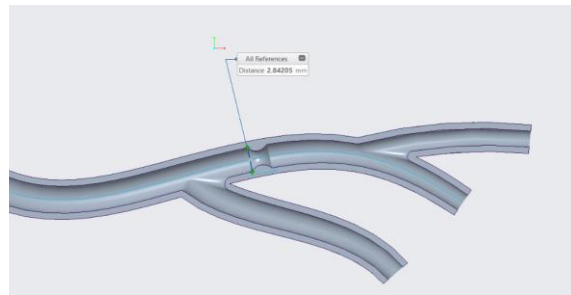


Fig. 9: Blockage in Left Anterior Descending (LAD) sub-arteries

A series of arterial blockage models were designed to study the effects of varying levels of stenosis on blood flow dynamics. The 81% blockage model features an arterial diameter of 2.84 mm, with a central diametrical distance of 0.55 mm and a blockage length of 2.29 mm. In the 61% blockage model, the central diametrical distance increases to 1.1 mm, while the blockage length is reduced to 1.74 mm. The 48% blockage model further increases the central diametrical distance to 1.47 mm with a blockage length of 1.37 mm. Similarly, in the 35% blockage model, the central diametrical distance is 1.85 mm, and the blockage length is 0.99 mm. Lastly, the 19% blockage model represents the least severe case, with a central diametrical distance of 1.85 mm and a blockage length of 0.55 mm. A total of 15 models were developed, and Computational Fluid Dynamics (CFD) simulations using ANSYS Fluent will be carried out to analyse blood flow velocity and pressure variations at the blockage points. These simulations aim to provide a comprehensive understanding of hemodynamic changes due to arterial stenosis, aiding in the assessment of cardiovascular disease progression and potential treatment strategies.

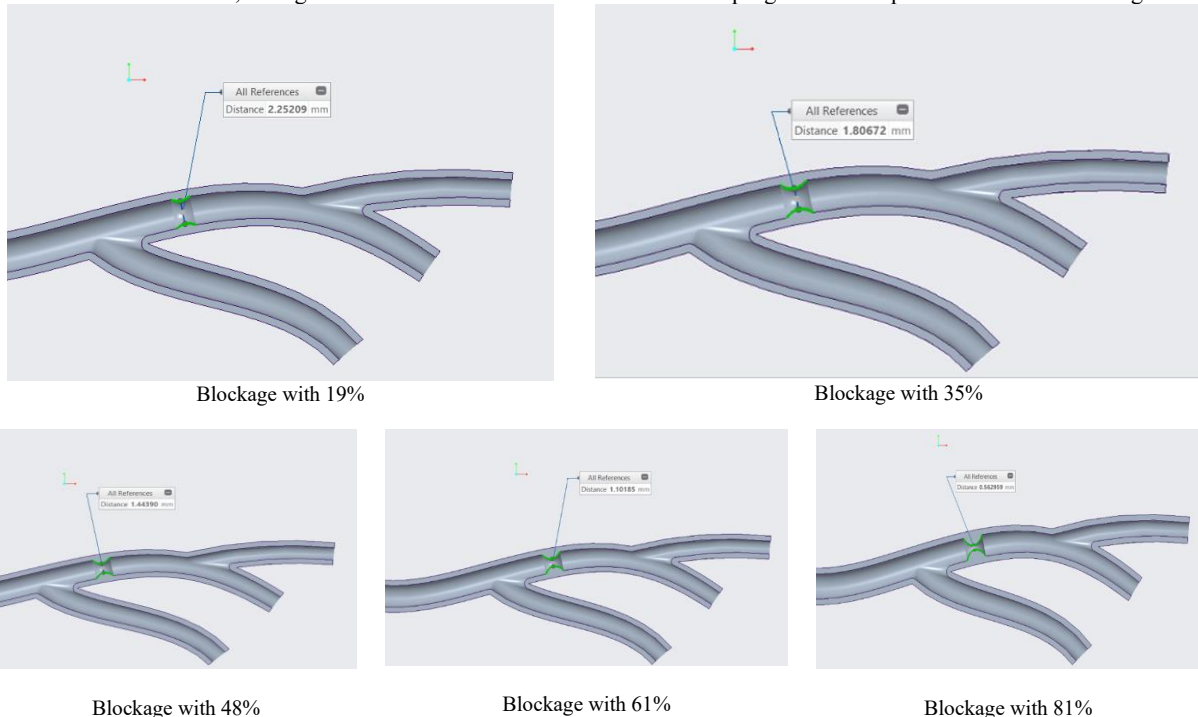


Fig. 10: Design models for varying percentages of blockages in sub-arteries, considering blockage levels of 81%, 61%, 48%, 35%, and 19%.

4. Analytical and CFD Analysis of Coronary Arteries

4.1 Analytical Analysis of blood flow through blockage

For the analytical analysis of blood flow through the arteries the parameter is considered as velocity and pressure of blood at normal condition. The schematic diagram of arteries with blockage is shown in figure 11 and the technical parameters are given in table 3.

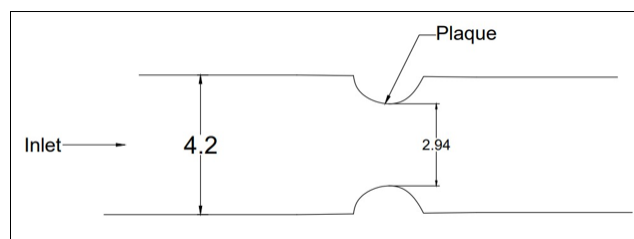


Fig. 11: 2D design of Plaque in Arteries

Table 3: Normal parameters of Blood At Normal Condition Blood Parameters

Parameter	Symbol	Unit	Value	Unit in meter	Value
Pressure	P	mmhg	80	N/m ²	10665.8
Velocity	V	m/s	0.3	m/s	0.3
Density	ρ	Kg/m ³	1060	Kg/m ³	1060
Diameter of Artery	D ₁	mm	4.2	m	0.0042
Diameter at plaque	D ₂	mm	2.94	m	0.00294

Using continuity equation, the velocity at plaque has been calculating with the given technical parameters. The velocity at plaque is obtained as 0.428571 m/s for the area of 0.013195 m² at normal artery and 0.009236 m² at plaque section. Shown in table 5.

By Continuity Equation

Equation: $A_1 \cdot V_1 = A_2 \cdot V_2$

Were,

A₁ = Area of cross section 1

V₁ = Velocity at section 1

A₂ = Area of cross section 2

V₂ = Velocity at section 2

Table 4: Parameter of blood flow through blockage

Parameter	Symbol	Unit in meter	Value
Pressure	P	N/m ²	10665.8
Velocity	V	m/s	0.3
Density	ρ	Kg/m ³	1060
Diameter of Artery	D ₁	m	0.0042
Diameter at plaque	D ₂	m	0.00294

Calculation of velocity at plaque

Table 5: Analytical Analysis of velocity

Parameter	Symbol	Unit	Value
Area of normal artery	A ₁	m ²	0.013195
Area of plaque section	A ₂	m ²	0.009236
Velocity at plaque	V ₂	m/s	0.428571

By Bernoulli's Equation

Equation: $P_1 + 1/2 \rho \cdot (V_1)^2 = P_2 + 1/2 \rho \cdot (V_2)^2$

Were,

P₁ = Pressure at section 1

V₁ = Velocity at section 1

P₂ = Pressure at section 2

V₂ = Velocity at section 2

ρ = Density of fluid flow

Calculation of pressure at plaque

Table 6: Analytical Analysis of pressure

Parameter	Symbol	Unit in meter	Value
Pressure	P ₁	N/m ²	10665.76
Velocity	V ₁	m/s	0.3
Density	ρ	Kg/m ³	1060
Velocity at plaque	V ₂	m/s	0.428571
Pressure at plaque	P ₂	N/m ²	10616.113
		mmhg	79.6276

From the analytical calculation the velocity at the blockage is 0.428 m/s and pressure is 10616.113 N/m².

4.3 Case Model Analysis

For analysis CFD Fluent is used, the CAD data of model is imported and analysis is carried out.

Meshing:

The Tetrahedral type meshing is done for all the models. As shown in Figure 12 the mesh is generated.

The blood flow path, boundary condition and material of blood and artery are taken from the fluid website and research papers.

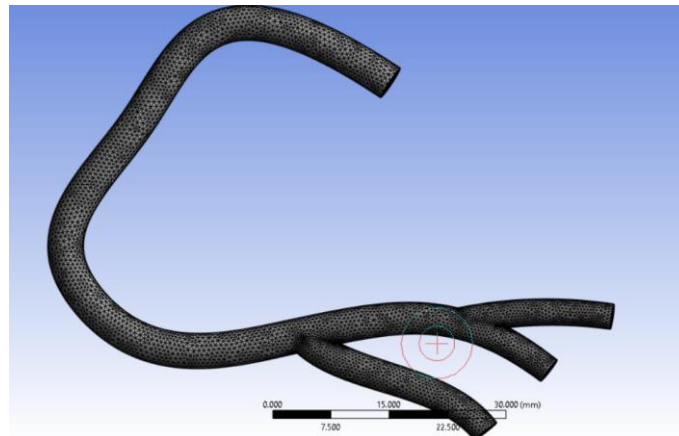


Fig. 12: Meshing of models

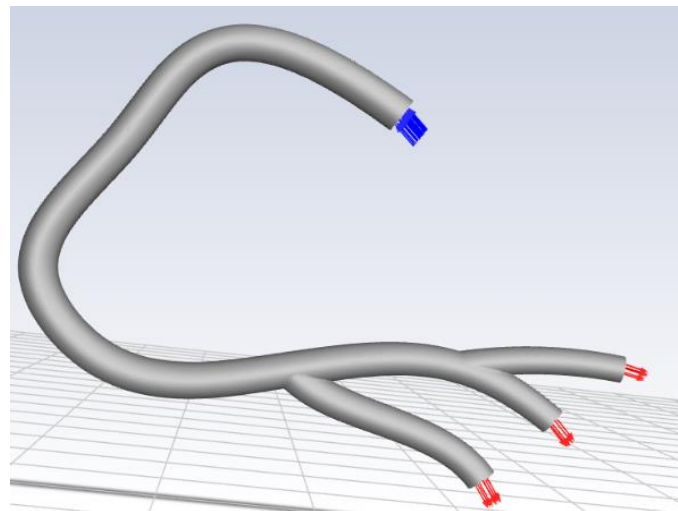


Fig. 13: Blood Flow setup

The material properties considered for blood and artery are taken from its foundation fluid website. The properties of blood are shown in table 7 and properties of artery is shown in table 8.

Table 7: Properties of Blood

Properties	Unit	Value
Density	Kg/m ³	1060
Specific Heat	J/(kg K)	3617
Thermal Conductivity	W/(Mk)	0.45
Viscosity	Kg/ms	0.004

Table 8: Properties of Artery

Properties	Unit	Value
Density	Kg/m ³	1300
Specific Heat	J/(kg K)	3306
Thermal Conductivity	W/(Mk)	0.46

4.3.1 Case model blood flow velocity analysis.

The velocity of blood flow at the point of blockage varies significantly based on the percentage of arterial obstruction. With 35% blockage, the inlet velocity of 0.3 m/s results in a maximum velocity of 0.81 m/s at the blockage site. In the case of 81% blockage, the same inlet velocity leads to a sharp increase in maximum velocity, reaching 8.96 m/s, indicating severe flow acceleration due to the narrowed passage. For 61% blockage, the maximum velocity rises to 2.23 m/s, while 48% blockage results in a maximum velocity of 1.34 m/s. The least severe condition, 19% blockage, experiences the smallest velocity change, with a peak velocity of 0.63 m/s. These findings highlight the significant impact of arterial narrowing on blood flow dynamics, where increased blockage results in higher velocity gradients, potentially leading to turbulent flow and increased shear stress on arterial walls.

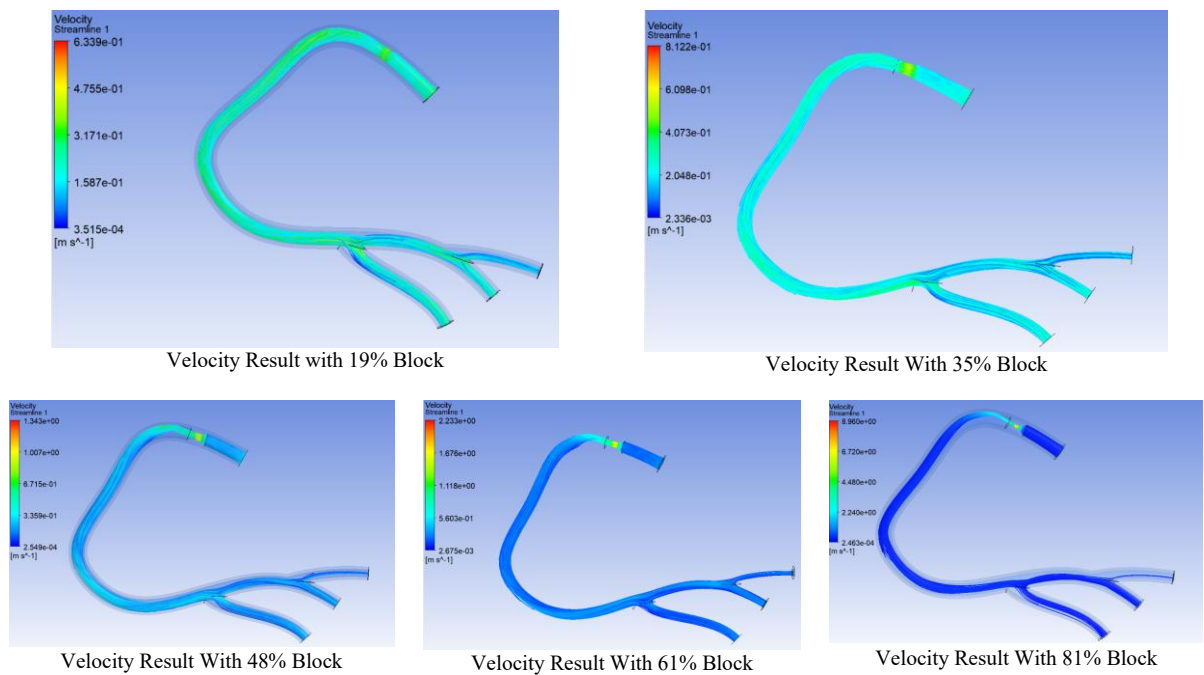


Fig. 14: Velocity of blood for blockages at the beginning of artery for various percentage of blockages

4.3.2 Case 2 blood flow velocity analysis

The velocity of blood flow at the blockage site varies depending on the severity of arterial narrowing when blockages are positioned before the branches. In the case of 81% blockage, an inlet velocity of 0.3 m/s results in a significant increase, reaching a maximum velocity of 7.91 m/s at the blockage. With 61% blockage, the maximum velocity observed is 2.25 m/s, while for 48% blockage, it is 1.32 m/s. A 35% blockage leads to a more moderate velocity increase, with a peak of 0.80 m/s, whereas the 19% blockage shows the least impact, with a maximum velocity of 0.60 m/s. These results demonstrate that higher blockages drastically alter blood flow dynamics, potentially leading to turbulent flow, increased shear stress, and higher risks of complications.

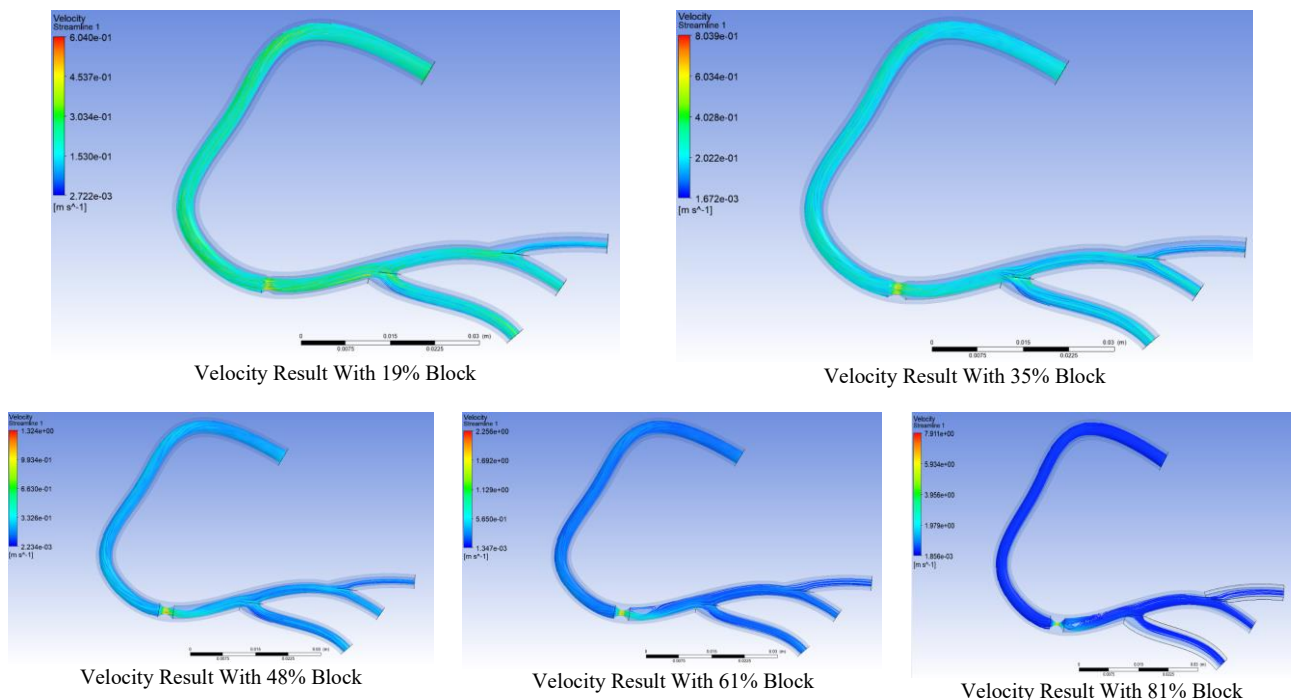


Fig. 15: Velocity of blood for blockages before sub-artery for various percentage of blockages

4.3.3 Case 3 blood flow velocity analysis

Velocity Result of blockages are placed after the branch. The velocity at the blockage site varies depending on the severity of the arterial narrowing. With 81% blockage, the inlet velocity of 0.3 m/s increases significantly to a maximum of 1.06 m/s at the blockage, indicating substantial acceleration due to the narrowed passage. For 61% blockage, the velocity at the blockage is 0.87 m/s, while for 48% blockage, it reduces to 0.70 m/s. In cases of 35% blockage, the velocity reaches 0.54 m/s, and for 19% blockage, it is slightly lower at 0.53 m/s. These results highlight how higher blockages significantly

impact blood flow dynamics, increasing velocity at the constriction site, which could contribute to shear stress and potential damage to the arterial walls.

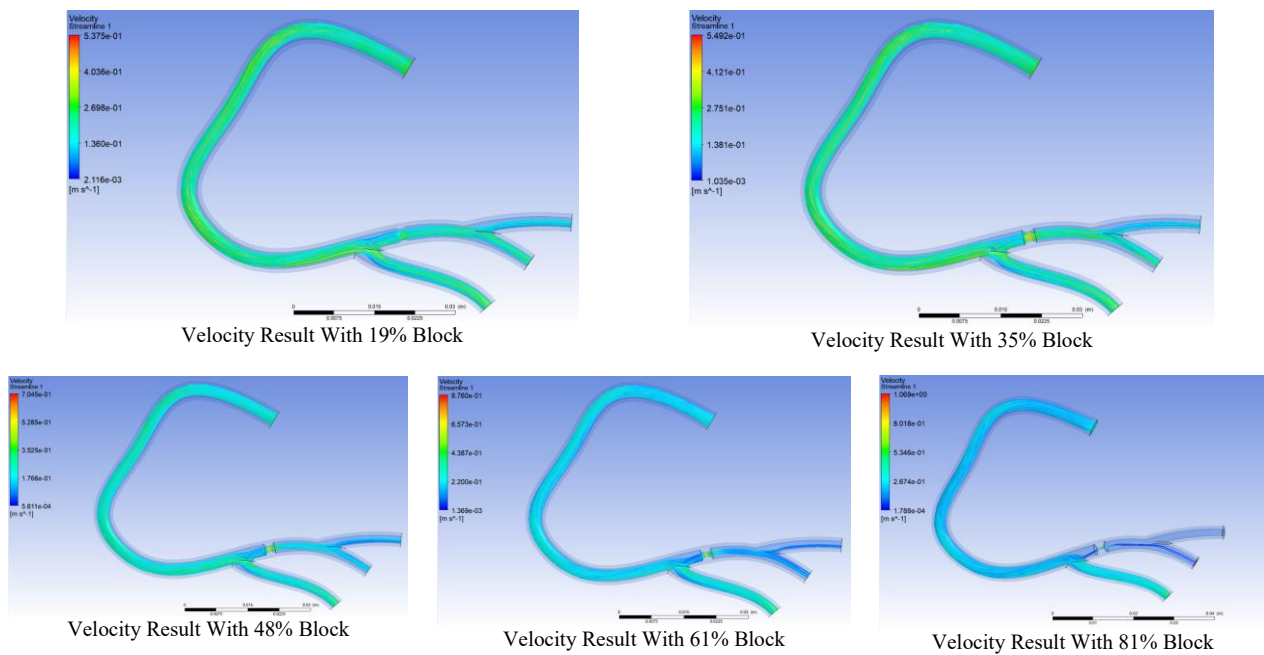


Fig. 16: Velocity of blood for blockages under sub-artery for various percentage of blockages

4.3.4 Case model Pressure analysis.

The pressure generated at the blockage site varies significantly depending on the severity of the arterial narrowing. With 35% blockage, the pressure at the blockage is 1.030×10^3 N/m², while for 81% blockage, it rises sharply to 2.88×10^4 N/m², indicating a substantial increase in pressure due to the restricted flow. In the case of 61% blockage, the pressure reaches 2.5×10^3 N/m², whereas for 48% blockage, it is slightly lower at 1.305×10^3 N/m². The most non-obstructive situation, 19% obstruction, generates the lowest pressure of 7.787×10^2 N/m². These results demonstrate the direct relationship between the extent of arterial obstruction and the pressure increase, highlighting the likelihood of elevated cardiovascular risks in instances of extreme narrowing.

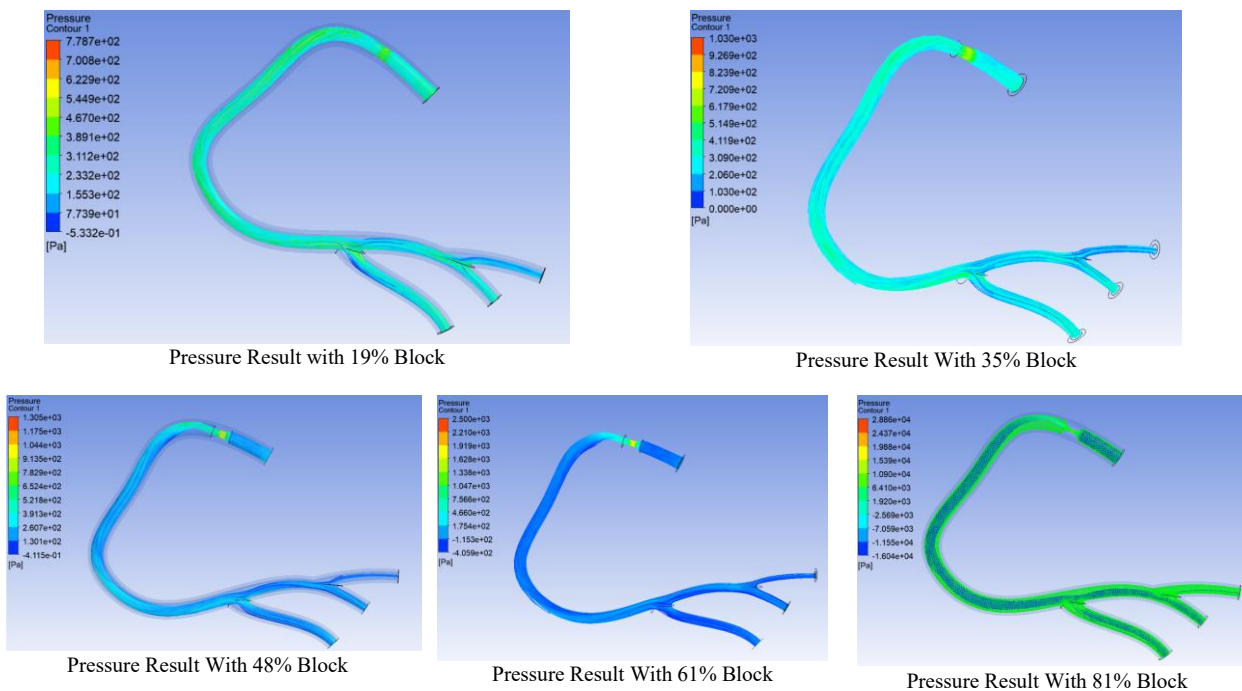


Fig. 17: Pressure due to blockages at the beginning of artery for various percentage of blockages

4.3.5 Case 2 Pressure analysis

The pressure developed at the site of blockage is quite different based on the degree of narrowing of the arteries. With 81% narrowing, the pressure at the constriction is 1.914×10^4 N/m², which is quite high due to the high level of restriction of blood flow. With 61% narrowing, the pressure decreases to 2.406×10^3 N/m², and with 48% narrowing, it is 1.362×10^3 N/m². For 35% blockage, the pressure is further decreased to 1.019×10^3 N/m², and for 19% blockage, it is lowest at 9.451×10^2 N/m². These findings depict the linear relationship between

severity of blockage and pressure increase, with increased blockages resulting in very high pressure levels, which can be a cause of enhanced cardiovascular risk.

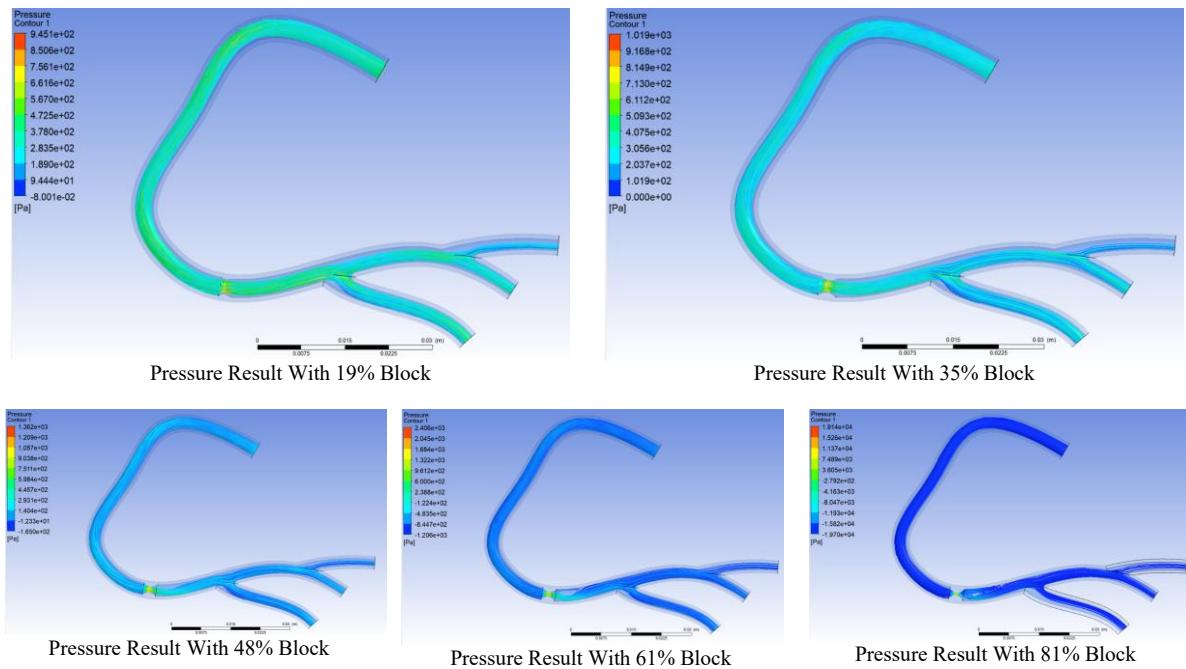


Fig. 18: Pressure due to blockages before sub-artery for various percentage of blockages

4.3.6 Case 3 Pressure analysis

When blockages are placed after the branches, the pressure at the blockage site follows a decreasing trend with reduced severity of arterial narrowing. For 81% blockage, the pressure at the constriction is $1.285 \times 10^3 \text{ N/m}^2$, which is significantly lower than when blockages are placed before the branches. For 61% blockage, the pressure is $1.094 \times 10^3 \text{ N/m}^2$, while for 48% blockage, it further reduces to $9.928 \times 10^2 \text{ N/m}^2$. In the case of 35% blockage, the pressure is $9.5 \times 10^2 \text{ N/m}^2$, and for 19% blockage, it is the lowest at $9.242 \times 10^2 \text{ N/m}^2$. These results suggest that the placement of blockages after arterial branches leads to a more distributed pressure drop, highlighting the importance of arterial geometry in hemodynamic behaviour.

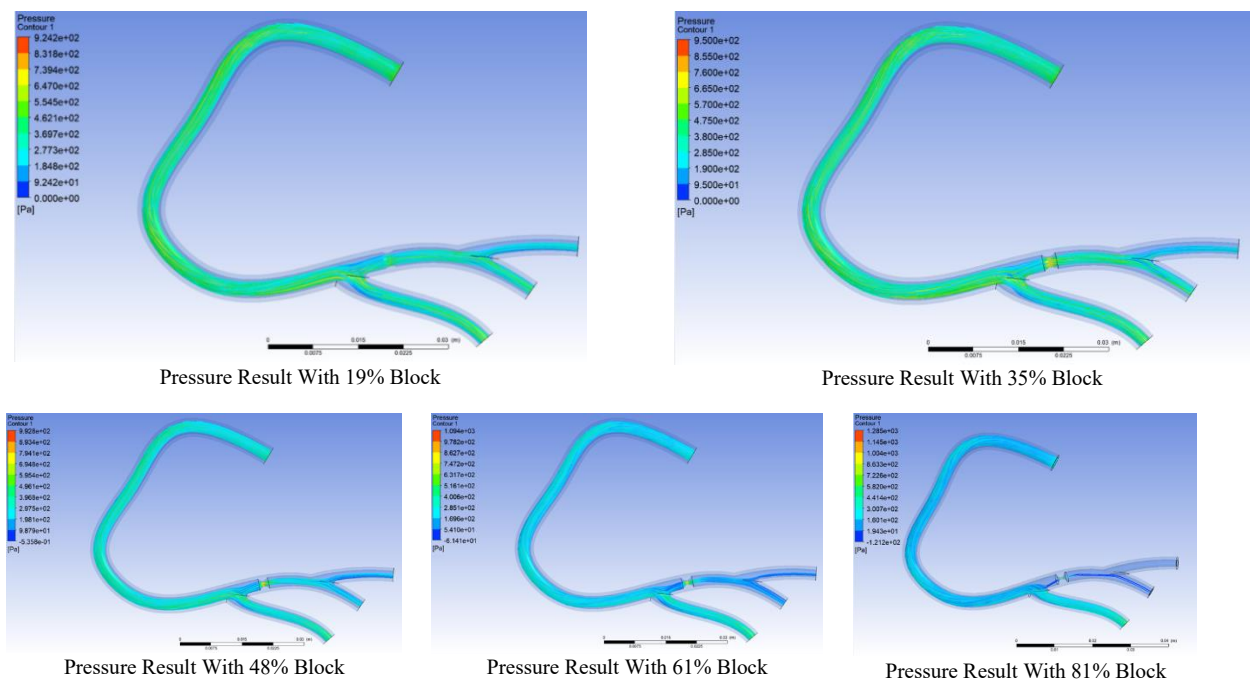


Fig. 19: Pressure due to blockages under sub-artery for various percentage of blockages

From analysis the velocity and the pressure are analysed at the point of the blockages, so in table 9 shows the result of case first, in which blockage is consider at starting point of the LAD artery it is as per the case of the patient. In table 10 shows the analysis result as blockage position is changed, blockage consider before the branches it is case 2. In case 3 the blockage position is after the branch as result of analysis is shown in table 11.

Table 9: Velocity and Pressure result at the blockage of the case 1.

Design Model	Diameter Gap	Blockage	Percentage of Block	Velocity	Unit	Pressure	Unit
LAD 0.6 mm	0.6	2.5	81	8.96	m/s	2.88×10^4	N/m ²
LAD 1.2 mm	1.2	1.9	61	2.23	m/s	2.5×10^3	N/m ²
LAD 1.6 mm	1.6	1.5	48	1.34	m/s	1.305×10^3	N/m ²
LAD 2.0 mm	2.0	1.1	35	0.81	m/s	1.030×10^3	N/m ²
LAD 2.5 mm	2.5	0.6	19	0.63	m/s	7.787×10^2	N/m ²

Table 10: Velocity and Pressure result at the blockage at different position (Case 2 Before the branches)

Design Model	Diameter Gap	Blockage	Percentage of Block	Velocity	Unit	Pressure	Unit
LAD 0.6 mm	0.6	2.5	81	7.91	m/s	1.91×10^4	N/m ²
LAD 1.2 mm	1.2	1.9	61	2.25	m/s	2.4×10^3	N/m ²
LAD 1.6 mm	1.6	1.5	48	1.32	m/s	1.362×10^3	N/m ²
LAD 2.0 mm	2.0	1.1	35	0.803	m/s	1.019×10^3	N/m ²
LAD 2.5 mm	2.5	0.6	19	0.604	m/s	9.45×10^2	N/m ²

Table 11: Velocity and Pressure result at the blockage at different position (Case 3 After the branches)

Design Model	Diameter Gap	Blockage	Percentage of Block	Velocity	Unit	Pressure	Unit
LAD 0.55 mm	0.55	2.29	81	1.06	m/s	1.28×10^3	N/m ²
LAD 1.1 mm	1.1	1.74	61	0.87	m/s	1.09×10^3	N/m ²
LAD 1.45 mm	1.47	1.37	48	0.704	m/s	9.92×10^2	N/m ²
LAD 1.8 mm	1.85	0.99	35	0.54	m/s	9.5×10^2	N/m ²
LAD 2.25 mm	2.29	0.55	19	0.53	m/s	9.24×10^2	N/m ²

5. Results and Discussion

By considering case study, the analytical calculation is carried out and the velocity at the section of plaque increase up to 0.42875 m/s and pressure drop is 10616.11 N/m². Shown in table 12.

For Sample model, the normal parameter is considered as water flowing through pipe and Velocity analysis is done with CFD. Table 12 shows the result.

Analytical Calculation Result

Table 12: Analytical model calculation result

Parameter	Symbol	Unit	Value
Velocity at inlet	V ₁	m/s	0.3
Pressure at inlet	P ₁	N/m ²	10665.76
Velocity at plaque	V ₂	m/s	0.42857
Pressure at plaque	P ₂	N/m ²	10616.11

Analytically the velocity and pressure at the blockage is 0.4285 m/s and 10616.11 N/m².

By considering case study the different percentages of blockages are created with the case, an analysis of model with velocity and pressure is carried out.

In table 13, the cases analysis result of velocity and pressure are shown. The three cases are created by changing position of blockage and by varying the percentage of blockage, In case 1 for lowest percentage of blockage which is 19% the velocity is 0.63 m/s and pressure is 778.7 N/m² and for highest percentage of blockage which is 81% the velocity is 8.96 m/s and pressure is 28800 N/m². In case 2 for lowest percentage of blockage which is 19% the velocity is 0.604 m/s and pressure is 945 N/m² and for highest percentage of blockage which is 81% the velocity is 7.91 m/s and pressure is 19100 N/m². In case 3 for lowest percentage of blockage which is 19% the velocity is 0.53 m/s and pressure is 924 N/m² and for highest percentage of blockage which is 81% the velocity is 1.06 m/s and pressure is 1280 N/m².

Table 13: Velocity and Pressure result at the blockage for different cases.

Cases	Design Model	Blockage	Percentage of Block	Velocity	Unit	Pressure	Unit
Case 1	LAD 0.6 mm	2.5	81	8.96	m/s	2.88×10^4	N/m ²
	LAD 1.2 mm	1.9	61	2.23	m/s	2.5×10^3	N/m ²
	LAD 1.6 mm	1.5	48	1.34	m/s	1.305×10^3	N/m ²
	LAD 2.0 mm	1.1	35	0.81	m/s	1.030×10^3	N/m ²
	LAD 2.5 mm	0.6	19	0.63	m/s	7.787×10^2	N/m ²
Case 2	LAD 0.6 mm	2.5	81	7.91	m/s	1.91×10^4	N/m ²
	LAD 1.2 mm	1.9	61	2.25	m/s	2.4×10^3	N/m ²
	LAD 1.6 mm	1.5	48	1.32	m/s	1.362×10^3	N/m ²
	LAD 2.0 mm	1.1	35	0.803	m/s	1.019×10^3	N/m ²
	LAD 2.5 mm	0.6	19	0.604	m/s	9.45×10^2	N/m ²
Case 3	LAD 0.55 mm	2.29	81	1.06	m/s	1.28×10^3	N/m ²
	LAD 1.1 mm	1.74	61	0.87	m/s	1.09×10^3	N/m ²
	LAD 1.45 mm	1.37	48	0.704	m/s	9.92×10^2	N/m ²
	LAD 1.8 mm	0.99	35	0.54	m/s	9.5×10^2	N/m ²
	LAD 2.25 mm	0.55	19	0.53	m/s	9.24×10^2	N/m ²

In table 14 shows the result of analysis at 81% of blockage which is consider as critical stage of blockage. Result shows as for case 1 the velocity is 8.96 m/s and pressure is 28800 N/m², for case 2 velocity is 7.91 m/s and pressure is 19100 N/m², for case 3 velocity is 1.06 m/s and pressure is 1280 N/m². So at the blockages the velocity of blood increases and pressure gets drops. For case 1 and case 2 velocity and pressure is approximately equal to each, but for case 3 velocity and pressure is not increases drastically, because the blockage is consider after the branch. So blood can flow through other branches so it does not affect much in the branches.

Table 14: Velocity and Pressure result at the blockage for diameter gap of 0.6mm

Cases	Design Model	Blockage	Percentage of Block	Velocity	Unit	Pressure	Unit
Case 1	LAD 0.6 mm	2.5	81	8.96	m/s	2.88×10^4	N/m ²
Case 2	LAD 0.6 mm	2.5	81	7.91	m/s	1.91×10^4	N/m ²
Case 3	LAD 0.55 mm	2.29	81	1.06	m/s	1.28×10^3	N/m ²

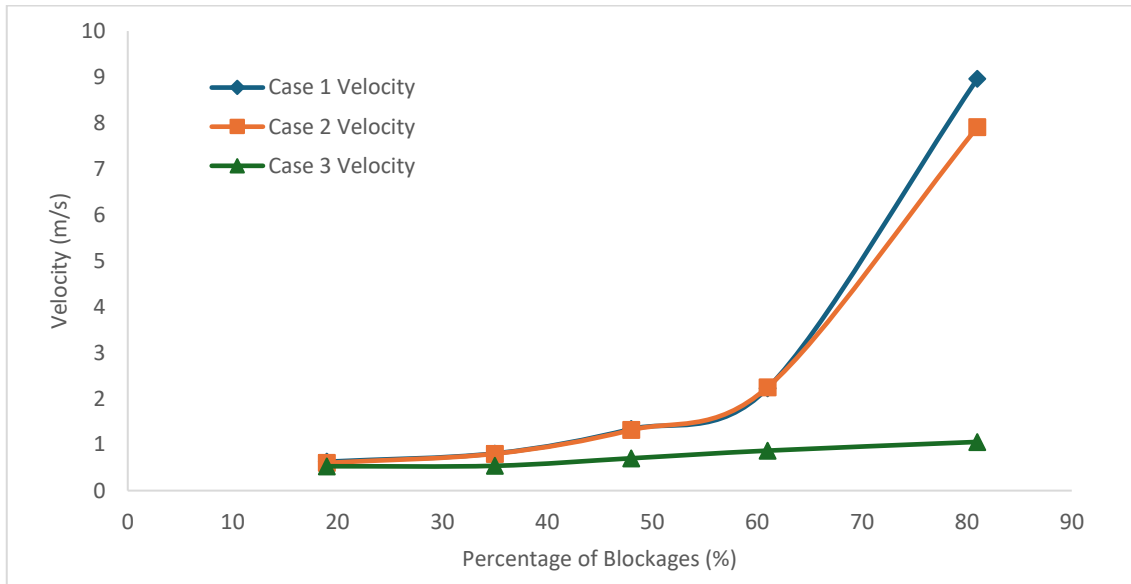


Fig. 20: Graphical representation of the velocity for each cases

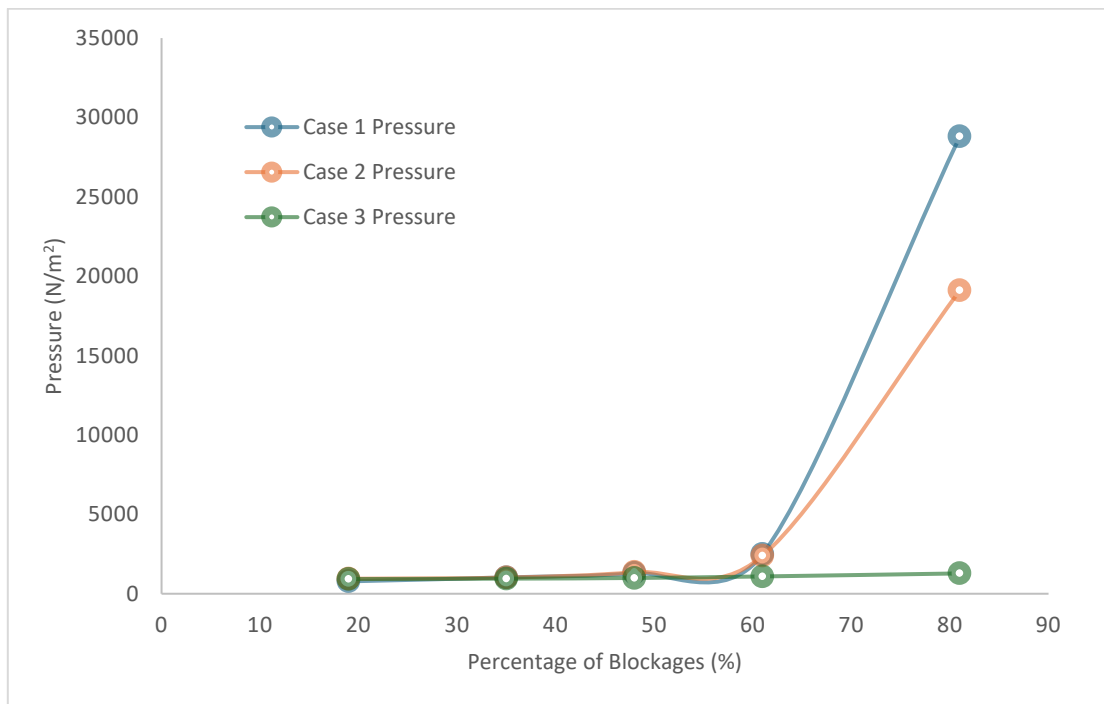


Fig. 21: Pressure Graph of cases

6. Conclusion

Based on the analysis carried out for the blockage in artery as per the case study of patient, it has been observed that the velocity at the section of plaque increase up to 0.42875 m/s and pressure drop is 10616.11 N/m². The same case is considered in the CFD analysis, and the velocity and pressure drop is check. For the validation of the pressure and velocity in blockages the position of blockage is change and total 15 model are considered to check the pressure drop and velocity flow at blockage which may be useful for the medical officer during surgery. The analysis has been carried out for diameter gap of 0.6mm to 2.5mm, so based on the analysis carried out it has been observed that velocity has been increases gradually from 0.53 m/s to 1.06 m/s at case 3 and in case 1 it is from 0.63m/s to 8.96m/s. So it indicates that the blockages in main branch affect the human body and blockages in branches will not affect much as the blood pass through different branches. In this work, the effect of blockages in the Left artery has been studied on hemodynamic changes at the locations of plaques and with varying the percentages of the blockages inside the coronary artery. There is a direct effect of plaques in the artery on hemodynamic changes such as recirculation flow, low flow velocity regions, and pressure gradient, indicating the potential for plaques to rupture, causing atherosclerosis.

Future research can explore a more detailed analysis of wall shear stress and pressure wave propagation to enhance the understanding of blood flow dynamics. Additionally, further studies on different boundary conditions can provide insights into their impact on simulation accuracy. A comparative study of blood flow simulation in veins and arteries can help in understanding the differences in hemodynamic behaviour between the two. Moreover, the development of various models incorporating different types of blockages in different arteries can serve as a valuable reference for medical professionals. Such models can act as standard reports, assisting healthcare practitioners in diagnosing and treating various cases more effectively.

References

- [1] Dwidmuthu P D, Mathpati C S, and Joshi J B (2018) CFD simulation of blood flow inside the human artery: Aorta. *Fluid Mechanics and Fluid Power*, FMFP2017–PAPER NO. 679.
- [2] Chaichana T, Sun Z, and Jewkes J (2012) Computational fluid dynamics analysis of the effect of plaques in the left coronary artery. *Computational and Mathematical Methods in Medicine* 2012: Article ID 504367.
- [3] Hannun R M, and Muhseen S J (n.d.) Computational fluid dynamic analysis of blood flow into normal right coronary artery in different patients. *Journal of Mechanical Engineering Research and Developments* 43(5): 460–471.
- [4] Sahu N, Sharma A, and Kumar P (2021) A numerical analysis of blood flow in clogged artery. *Journal of Physics* 1964(6): 062102.
- [5] Carvalho V, Pinho D, Lima R A, Teixeira J C, and Teixeira S (2021) Blood flow modeling in coronary arteries. *MDPI* 6: 53.
- [6] J N K, Mathew L, and Karnan H (2018) Blood hammer model-modeling and analysis of coronary artery with vascular occlusion using computational fluid dynamics analysis. *International Journal of Engineering Research & Technology* 6(07).
- [7] Doost S N, Ghista D, Su B, Zhong L, and Morsi Y S (2016) Heart blood flow simulation. *BioMedical Engineering* 15: 101.
- [8] Morris P D, Lawford P V, Hose D R, Narracott A, Gunn J P, and Gunn J (2016) Computational fluid dynamics modelling in cardiovascular medicine. *Heart* 102: 18–28.
- [9] Barzegar Y, and Barzegar A (2021) Computational fluid dynamic (CFD) simulation of bifurcate artery.
- [10] Long W, Zhang Y, Feng X, and Li Y (2021) Investigation of the effect of arteriole clogging of the heart on the characteristics of intravenous blood flow.
- [11] Pandey R, Kumar M, and Srivastav V K (2019) Comparison of blood flow in normal and plaque coronary models using numerical simulation. In *International Conference on Sustainable Computing in Science, Technology & Management*.
- [12] Sheth V, and Ritter A (2010) Using computational fluid dynamics model to predict changes in velocity properties in stented carotid artery. In *COM-SOL Conference*.
- [13] Kim H J, Vignon-Clementel I E, Coogan J S, Figueroa C A, Jansen K E, and Taylor C A (2010) Patient-specific modeling of blood flow and pressure in human coronary arteries. *Annals of Biomedical Engineering* 38(10).
- [14] Surigala N (2015) CFD analysis of blood flow through stenosed arteries. *Graduate Research Theses & Dissertations*, p. 1711.
- [15] Alhassen M, Abdalla A, Ali T, and Akeel M (2021) Variations in diameter of the left coronary artery and its main branches among adult population of Khartoum State, Sudan. *Journal of Hypertension and Cardiology*. ISSN: 2329-9487.
- [16] IT*IS Foundation (2025) Tissue properties overview. Available online: <https://itis.swiss/virtual-population/tissue-properties/overview/>.
- [17] Cleveland Clinic (2025) Coronary artery disease. Available online: <https://my.clevelandclinic.org/health/diseases/16898-coronary-artery-disease>.
- [18] Cardiovascular Consultants PC (2025) Atherosclerotic heart disease. Available online: <https://www.cardiovascularconsultantspc.com/services-specialties/tests-and-procedures/atherosclerotic-heart-disease/>.
- [19] Kumbhalkar M A, Rambhad K S, and Nand Jee K (2021) An insight into biomechanical study for replacement of knee joint. *Materials Today: Proceedings* 47(11): 2957–2965.
- [20] Kumbhalkar M A, Rambhad K S, and Nand Jee K (2021) An insight into biomechanical study for replacement of knee joint. *Materials Today: Proceedings*. <https://doi.org/10.1016/j.matpr.2021.05.202>.
- [21] Khamankar S D, Ade N K, Sahare P H, Kumbhalkar M A, Rambhad K S, Choudhari S A, Bhise D V, and Sardeshmukh M M (2023) CFD analysis of a butterfly valve to optimize its design. *AIP Conference Proceedings* 2839. <https://doi.org/10.1063/5.0167691>.
- [22] Sahare P H, Ade N K, Kumbhalkar M A, Rambhad K S, Giradkar C, Gandate J, Badkelwar S, and Sondawale S (2023) Comparison of alternative fuels in single cylinder diesel engine using CFD. *AIP Conference Proceedings* 2839. <https://doi.org/10.1063/5.0167692>.